SMART 2023

Smart Structures and Materials

Proceedings of the 10th International Conference on Smart Structures and Materials
Held in Patras, Greece
3-5 July 2023

Edited by:

Dimitris Saravanos
University of Patras, Greece

Ayech Benjeddou
ISAE-SUPMECA & SUA-UTC ROBERVAL, France

Nikos Chrysochoidis
University of Patras, Greece

Theodosis Theodosiou
University of Thessaly, Greece

A publication of:

Mechanical Engineering & Aeronautics Department
University of Patras
Greece

X ECCOMAS Thematic Conference on Smart Structures and Materials
SMART 2023
D.A. Saravanos, A. Benjeddou, N. Chrysochoidis and T. Theodosiou (Eds)

SEMI-ACTIVE SLIDING-MODE CONTROL FOR LOCAL MITIGATION OF STRUCTURAL VIBRATIONS BY MEANS OF ON/OFF NODES

MARIUSZ OSTROWSKI, ALEKSANDRA JEDLIŃSKA, BŁAŻEJ POPŁAWSKI, BARTŁOMIEJ BŁACHOWSKI, GRZEGORZ MIKUŁOWSKI, DOMINIK PISARSKI, ŁUKASZ JANKOWSKI*

Institute of Fundamental Technological Research (IPPT PAN)
Polish Academy of Sciences
Pawińskiego 5B, 02-106 Warsaw, Poland
e-mail: ljank@ippt.pan.pl

Abstract. This contribution presents a sliding-mode control approach for the mitigation of vibrations in frame-like structures. The control is implemented in a semi-active manner, that is, without significant external control forces and substantial power consumption, which are typical for active control approaches. Here, the control is achieved through dynamic, low-cost modification of properties at selected structural nodes. The employed actuators have the untypical form of two-state hinges, which can switch between two extreme states: no transfer of bending moments (effectively a hinge) and full transfer of bending moments (a locked hinge or a typical frame node). Consequently, the control forces are dissipative and coupled to the response. Previous research in this area focused on purely energetic considerations, aiming for global damping of vibrations. In contrast, this paper formulates the control objective in terms of local displacements of a selected degree of freedom, which can be interpreted as the task of isolating it from external excitations. This formulation is employed to define the target sliding hyperplane. The state of the actuators is chosen such that the effective control forces push the structural state toward the target hyperplane. The approach is verified in a numerical example of a six-story shear-type structure subjected to random seismic excitation.

Key words: Structural control, Semi-active control, Sliding mode control, On/off nodes

1 INTRODUCTION

Structural vibrations result from operational conditions or extreme excitations and have adverse effects on the involved structures [1]. A prime example includes satellite structures, which tend to be extremely lightweight and flexible and thus excessively prone to prolonged vibrations [2]. Another example is civil engineering structures subjected to seismic excitations. Consequently, there is an ongoing, intense research effort in structural control [3, 4], where control techniques can be generally divided into passive, active, and semi-active approaches [5].

Passive approaches focus on designing structures to optimally absorb vibrational energy [6]. This is usually achieved through specialized dissipative elements [7], seismic isolation systems [8], and tuned mass dampers [9]. Active approaches employ actuators that generate external control forces, which is effective [10] but entails considerable energy costs and can result in instabilities.

This contribution addresses semi-active control. Such approaches aim for optimal self-adaptation of the controlled structure and rely on real-time, low-cost modifications of its material or structural characteristics [11]. Good examples of employed actuators are semi-active mass dampers [12]. In many semi-active systems, control forces are solely dissipative, and the open-loop optimal control is of the bang–bang type. Consequently, the control problem is reduced to determining the switching surface [13, 14].

Unconventional semi-active actuators include various stiffness-switched elements in the form of slender bars with switchable axial stiffness [15] or structural joints with an on/off ability to transmit bending moments between adjacent beams [16]. Such joints are essentially friction-based lockable hinges, and early control laws aimed to stimulate local dissipation by maximizing nodal force–displacement hysteresis [17, 18]. However, these nodes can also be utilized to trigger the transfer of vibrational energy to high-order modes, which are more effectively damped by standard material damping mechanisms compared to low-order modes [19]. The control laws involved are either simple heuristics [20] or more formal and explicitly aimed at modal energy transfer [21]. These formulations focused on energetic measures of structural vibrations. However, energy is a suitable overall measure of the severity of structural vibrations but often does not correlate well with local vibration amplitudes. Therefore, this contribution presents an approach inspired by [21] that focuses on minimizing displacement in a particular degree of freedom (DOF). The sliding-mode control formulation is employed [22], and the sliding hyperplane is defined in the configuration space by zero displacement in the target DOF. The maximal switching frequency is constrained to account for the physical limits of the actuators and prevent chattering. Additionally, the state is temporarily switched just before reaching the target hyperplane, which is motivated by the optimal switching rules presented in [23].

2 ON/OFF NODE AND THE CONTROL METHOD

2.1 On/off node

The on/off node is designed to enable control of the transmission of bending moments between adjacent beams, see Fig. 1. In the finite element (FE) model, in addition to the two usual displacement DOFs x and y, the node also has two rotational DOFs denoted θ_1 and θ_2. During the FE model aggregation phase, the adjacent beams are allocated to either θ_1 or θ_2. The beams assigned to the same rotational DOF are rigidly connected with a full transmission of moments (beams A and B in Fig. 1). However, the transfer of bending moments between the two groups of beams, assigned respectively either to θ_1 (beam A and B) or to θ_2 (beam C), can be controlled by switching the hinge shown in the scheme between the locked and unlocked states. In the unlocked state, both rotational DOFs rotate independently. In the locked state, the hinge

implements a kinematic constraint of the following form: $\dot{\theta}_1 = \dot{\theta}_2$, which freezes the rotations and allows the moments to be transmitted between the involved beams.

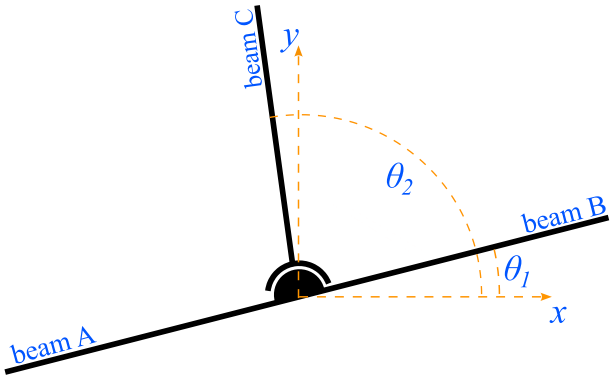

Figure 1: A controllable node

2.2 Equation of motion

The equation of motion for the controlled structure is expressed as follows:

$$\mathbf{M}\ddot{\mathbf{u}}(t) + \left(\mathbf{C} + \sum_i \gamma_i(t)\mathbf{C}_i\right)\dot{\mathbf{u}}(t) + \mathbf{K}\mathbf{u}(t) = \mathbf{f}(t), \tag{1}$$

where the vector $\mathbf{u}(t)$ collects the generalized displacements and $\mathbf{f}(t)$ denotes the excitation force. The matrices $\mathbf{M}$, $\mathbf{C}$, and $\mathbf{K}$ represent the mass, damping, and stiffness matrices, respectively. The function $\gamma_i(t) \in \{0, 1\}$ is the control signal of the ith controllable node. Finally, the matrix $\mathbf{C}_i$ implements the locking action for the ith node and represents a viscous damper of relative rotations between its two rotational DOFs:

$$\mathbf{C}_i = c_i\,\mathbf{L}_i \begin{bmatrix} 1 & -1 \\ -1 & 1 \end{bmatrix} \mathbf{L}_i^{\mathrm{T}}, \tag{2}$$

where c_i is a large coefficient, and $\mathbf{L}_i$ is the local-to-global ((θ_1, θ_2)-to-global) coordinate transformation matrix. The locking model relies on viscous damping. In dynamic analysis, it can be proven to reliably model a rigid connection with full transmission of bending moments [24].

2.3 Control forces

In Eq. (1), the control forces can be shown explicitly by moving the control terms from the left-hand side to the right-hand side:

$$\mathbf{M}\ddot{\mathbf{u}}(t) + \mathbf{C}\dot{\mathbf{u}}(t) + \mathbf{K}\mathbf{u}(t) = \mathbf{f}(t) - \sum_i \gamma_i(t)\mathbf{C}_i\dot{\mathbf{u}}(t). \tag{3}$$

These control forces are switched on and off by means of the control functions $\gamma_i(t) \in \{0, 1\}$. In modal coordinates $\boldsymbol{\xi}(t)$, defined as $\mathbf{u}(t) = \boldsymbol{\Phi}\boldsymbol{\xi}(t)$, where the matrix $\boldsymbol{\Phi}$ contains the modal vectors as columns, the control forces are expressed as follows:

$$\tilde{\mathbf{f}}_i(t) = -\boldsymbol{\Phi}^{\mathrm{T}}\mathbf{C}_i\boldsymbol{\Phi}\dot{\boldsymbol{\xi}}(t) = -\boldsymbol{\Phi}^{\mathrm{T}}\mathbf{C}_i\dot{\mathbf{u}}(t). \tag{4}$$

2.4 Sliding-mode control

The control objective is defined in terms of the displacement in a particular kth DOF:

$$u_k = \boldsymbol{\Phi}_k\boldsymbol{\xi} = 0, \tag{5}$$

where the column vector $\boldsymbol{\xi}$ denotes a point in the modal configuration space, and the row vector $\boldsymbol{\Phi}_k$ collects the modal amplitudes in the kth DOF. The proposed control aims to drive the modal displacements towards the target hyperplane. For each controllable node, its state is determined in such a way that the control forces, if activated, point toward the target hyperplane.

Let $\boldsymbol{\xi}(t)$ be the displacement vector in modal coordinates, and let $\Delta\boldsymbol{\xi}(t)$ represent the vector that points from $\boldsymbol{\xi}(t)$ perpendicularly towards the target hyperplane. It can be shows that

$$\Delta\boldsymbol{\xi}(t) = -u_k(t)\frac{\boldsymbol{\Phi}_{k\cdot}^{\mathrm{T}}}{\boldsymbol{\Phi}_{k\cdot}\boldsymbol{\Phi}_{k\cdot}^{\mathrm{T}}}. \tag{6}$$

The direction of the control forces $\tilde{\mathbf{f}}_i(t)$ (toward or outward the target hyperplane) can be determined based on the sign of the cosine between $\tilde{\mathbf{f}}_i(t)$ and $\Delta\boldsymbol{\xi}(t)$. Therefore, the initial candidate for the control law is:

$$\gamma_i(t) = H\left(\tilde{\mathbf{f}}_i(t)^{\mathrm{T}}\Delta\boldsymbol{\xi}(t)\right) = H\left(u_k(t)\boldsymbol{\Phi}_{k\cdot}\boldsymbol{\Phi}^{\mathrm{T}}\mathbf{C}_i\dot{\mathbf{u}}(t)\right), \tag{7}$$

where $H(\cdot)$ represents the Heaviside step function. This law is further modified by

1. *Constraining the maximal switching frequency of a controllable node*, which models the limitations of physical actuators and helps to prevent chattering [25]. For each node, it is assumed that the state switches must be separated by a time interval of at least Δt.

2. *Introducing a phase-related correction*. Inspired by the optimal switching rules investigated in [23, 13], the control forces defined in Eq. (7) are reversed when the modal displacement $\boldsymbol{\xi}(t)$ approaches the target hyperplane:

$$\alpha_i(t) = \begin{cases} 1 - H\left(u_k(t)\boldsymbol{\Phi}_{k\cdot}\boldsymbol{\Phi}^{\mathrm{T}}\mathbf{C}_i\dot{\mathbf{u}}(t)\right) & \text{if } 1 \le \psi(t) \le 1 + \kappa, \\ H\left(u_k(t)\boldsymbol{\Phi}_{k\cdot}\boldsymbol{\Phi}^{\mathrm{T}}\mathbf{C}_i\dot{\mathbf{u}}(t)\right) & \text{otherwise,} \end{cases} \tag{8}$$

   where $\kappa \in (0, 1)$ is a certain constant and $\psi(t)$ is related to the phase:

$$\psi(t) = \frac{2}{\pi}\arctan\left(u_k(t), \dot{u}_k(t)\right) \bmod 2. \tag{9}$$

3 NUMERICAL EXAMPLE

3.1 Six-story shear structure and seismic excitation

The proposed control approach is tested using a model of a six-story shear-type structure shown in Figure 2. The geometric and material characteristics of the structure are similar to those in [21]. Each story measures 0.4×0.4 m, and each beam has a cross-section of 8×10 mm. The material is steel (210 GPa, 7,860 kg/m^3). Twelve controllable nodes (1.2 kg) are placed in pairs at each story.

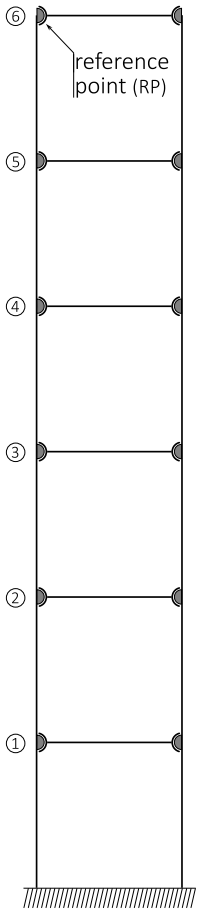

Figure 2: The simulated six-story shear-type structure, which is subjected to random seismic excitation. The control objective is to minimize the horizontal displacements of the reference point (RP)

Euler–Bernoulli beam FEs are used. The FE model has 54 DOFs, out of which 6 are fixed. The natural frequencies of the structure with all the nodes locked are 2.49, 7.75, 13.71, ..., 1724.89 Hz. If all nodes are unlocked, the natural frequencies decrease to 0.41, 2.56, 7.21, ..., 1756.95 Hz. A stiffness-proportional damping model is assumed with 1% damping ratio in the first mode of the structure with all nodes locked. If all nodes are unlocked, the damping ratio of the first node decreases proportionally to the natural frequency and equals only 0.16%.

The excitation force $\mathbf{f}(t)$ in Eq. (1) models a random seismic excitation:

$$\mathbf{f}(t) = -\mathbf{M}\boldsymbol{\ell}_{\mathrm{x}} a(t), \tag{10}$$

where $\mathbf{M}$ denotes the mass matrix, the binary vector $\boldsymbol{\ell}_{\mathrm{x}}$ selects the horizontal DOFs, and $a(t)$ is the ground acceleration. In each time step t_j the ground acceleration is an independently drawn from the normal distribution, $a(t_j) \sim N(0, 1)$. The two controllable nodes on each story are operated synchronously, so that they are always in the same state. Structural response is computed using the Newmark algorithm with $\alpha = 0.25$, $\delta = 0.5$, and the time step of 0.1 ms.

3.2 Responses

The two control parameters are chosen as $\kappa = 0.04$ and $\Delta t = 5$ ms, resulting in a maximum switching frequency of 100 Hz. The results are computed based on repeated simulations of a 20s-long time interval, each time with zero initial conditions. Quantitative assessment is performed both in the time domain (response rms) and in the frequency domain (FRF amplitude). In each considered case, 4000 simulations were performed. Eight cases are considered:

Case P: *Passive structure*, which serves the reference case and corresponds to the structure with all nodes locked (typical frame structure).

Case A: *All nodes controlled*. Nodes are controlled synchronously for each of the six stories. Accordingly, six independent control functions are computed and used.

Cases 1–6: *Single controlled story*. The nodes at only a selected story are controlled, while all other nodes are locked. There is a single control function in each of these six cases.

Fig. 3 presents example responses computed for Case P, Case A, and Case 3.

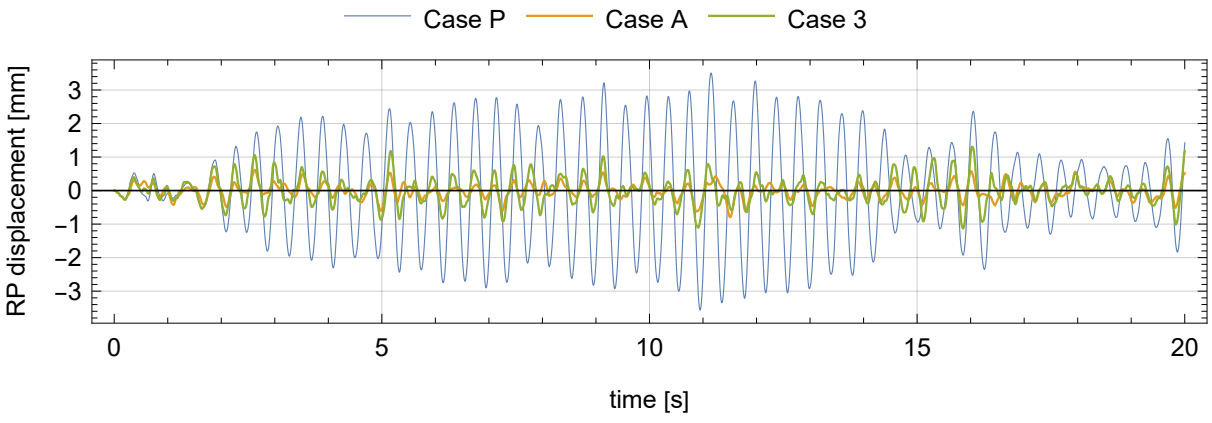

Figure 3: Example RP displacements computed for the same realization of the random seismic excitation in Case P, Case A, and Case 3

3.2.1 Statistics of the response rms

For each of the 4000 independently simulated random seismic excitations, the rms of the RP response was computed for the controlled structures (Cases A and 1–6) and then divided by the corresponding rms of the passive structure (Case P). The histograms of the resulting rms ratios are depicted in Fig. 4. The corresponding means and standard deviations are listed in Table 1.

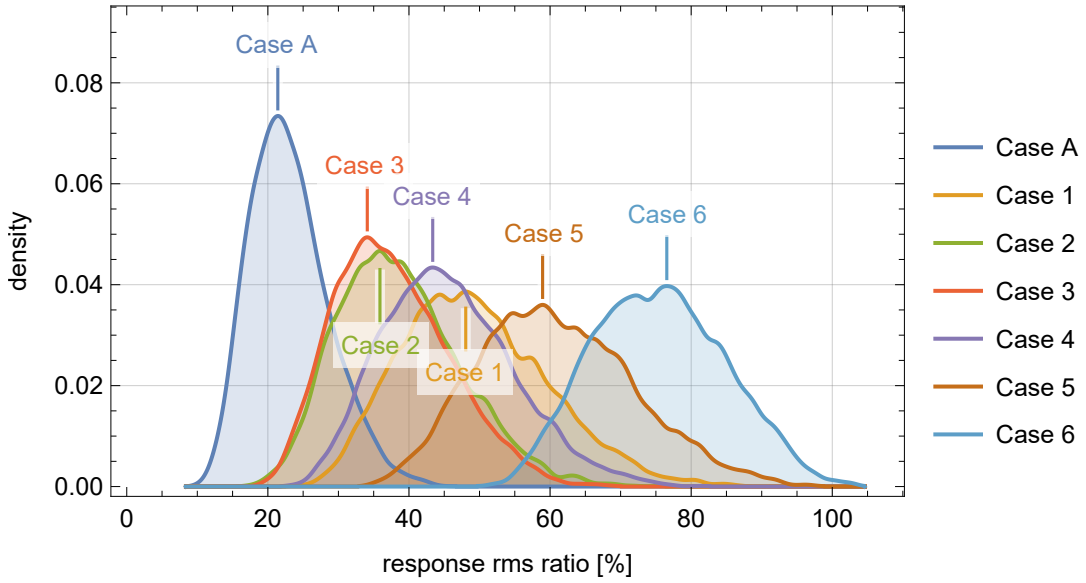

Figure 4: Histograms of the response rms ratios (controlled/passive) for the seven controlled cases

Table 1: Control effectiveness expressed in terms of the response ratios (controlled/passive): means and standard deviations of the time-domain response rms ratios and the 1st mode amplitude ratios

Case	A	1	2	3	4	5	6
rms ratio, mean [%]	23.08	49.33	38.66	37.63	45.63	60.88	75.48
rms ratio, std. dev. [%]	5.54	10.35	8.67	8.13	9.24	11.00	9.35
1st mode ampl. ratio, rms [%]	8.40	34.01	22.27	22.46	32.21	52.15	69.78
1st mode ampl. ratio, std. dev. [%]	3.44	14.12	9.31	9.09	13.06	19.55	18.42

3.2.2 Frequency-domain response

Figure 5 presents the mean amplitudes of the RP displacements computed for Case P (passive structure) and Case A (structure with all nodes controlled). The $\pm\sigma$ bands of one standard deviation are included. Figure 6 plots the mean amplitudes as computed for all cases: Case P, Case A, and Cases 1–6.

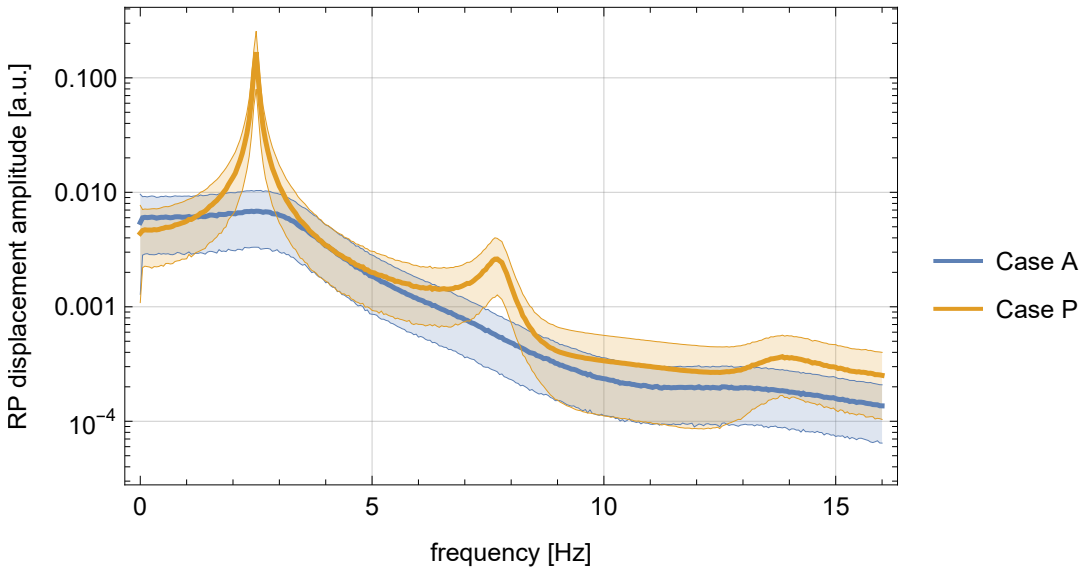

Figure 5: Frequency-domain amplitudes of the RP response computed for Case P and Case A: mean and $\pm\sigma$ band

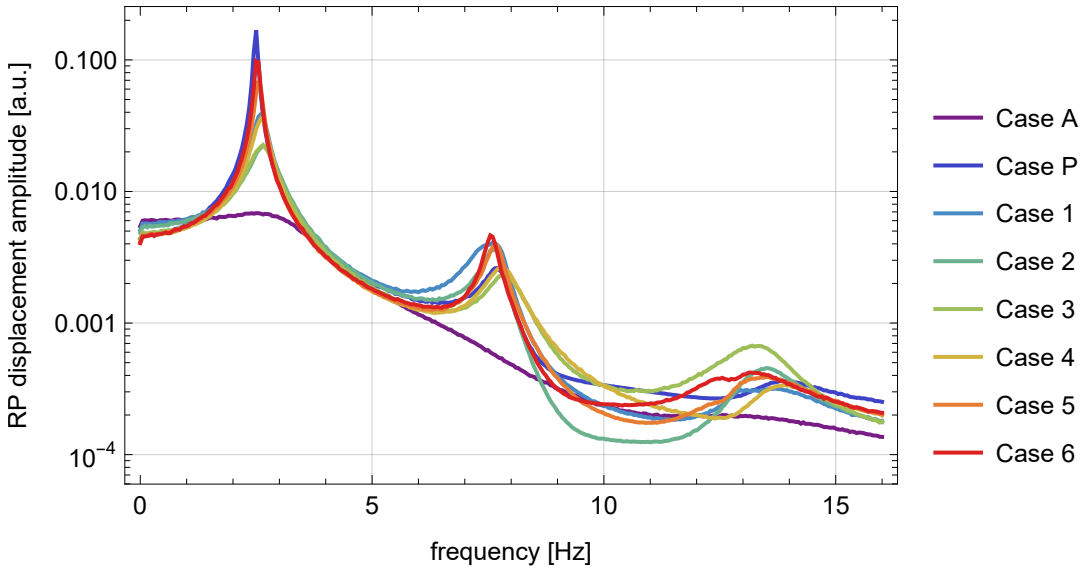

Figure 6: Frequency-domain mean amplitudes of the RP response for all cases

Figures 5 and 6 depict the amplitude in the frequency interval 0–16 Hz, which covers the three lowest natural frequencies of the structure. In all cases the first mode dominates the response. The two last rows of Table 1 list the basic statistics (means and standard deviations) of the corresponding amplitude ratios (controlled/passive) for all control Cases A and 1–6.

4 CONCLUSION

This contribution presents a semi-active sliding-mode control approach for mitigating vibrations in frame structures. Unconventional actuators are employed: two-state switchable nodes, essentially lockable hinges, that enable an on/off control of their ability to transmit bending moments between adjacent beams. In contrast to earlier approaches, which focused on energetic considerations, the proposed method concentrates on displacement response in a selected degree of freedom.

The approach was tested on a six-story shear-type structure subjected to random seismic excitation. The effectiveness was assessed statistically (means and standard deviations) in terms of the rms of the time-domain response, as well as the FRF amplitude. Depending on the number and placement of the actuators, the target response characteristics in the controlled structure were reduced to 23–76% of their values in the passive structure.

Near-term research tasks include applications to nonparametrically modeled structures [26] and modular structures [27], as well as adaptation, application, and evaluation in the context of reinforcement learning techniques [28].

5 ACKNOWLEDGEMENTS

This research was funded in whole or in part by the National Science Centre, Poland, under the grant agreement 2020/39/B/ST8/02615. For the purpose of Open Access, the authors have applied a CC-BY public copyright licence to any Author Accepted Manuscript (AAM) version arising from this submission.

REFERENCES

[1] B. Basu, O. S. Bursi, F. Casciati, S. Casciati, A. E. Del Grosso, M. Domaneschi, L. Faravelli, J. Holnicki-Szulc, H. Irschik, M. Krommer, M. Lepidi, A. Martelli, B. Ozturk, F. Pozo, G. Pujol, Z. Rakicevic, and J. Rodellar, "A European association for the control of structures joint perspective. Recent studies in civil structural control across Europe," *Structural Control and Health Monitoring*, vol. 21, no. 12, pp. 1414–1436, 2014.

[2] M. Sabatini, P. Gasbarri, R. Monti, and G. B. Palmerini, "Vibration control of a flexible space manipulator during on orbit operations," *Acta Astronautica*, vol. 73, pp. 109–121, 2012.

[3] B. Spencer Jr. and S. Nagarajaiah, "State of the art of structural control," *Journal of Structural Engineering*, vol. 129, no. 7, pp. 845–856, 2003.

[4] F. Casciati, J. Rodellar, and U. Yildirim, "Active and semi-active control of structures-theory and applications: A review of recent advances," *Journal of Intelligent Material Systems and Structures*, vol. 23, no. 11, pp. 1181–1195, 2012.

[5] T. E. Saaed, G. Nikolakopoulos, J.-E. Jonasson, and H. Hedlund, "A state-of-the-art review

of structural control systems," *JVC/Journal of Vibration and Control*, vol. 21, no. 5, pp. 919–937, 2015.

[6] Y. Parulekar and G. Reddy, "Passive response control systems for seismic response reduction: A state-of-the-art review," *International Journal of Structural Stability and Dynamics*, vol. 9, no. 1, pp. 151–177, 2009.

[7] Z. M. Pawlak and R. Lewandowski, "The effectiveness of the passive damping system combining the viscoelastic dampers and inerters," *International Journal of Structural Stability and Dynamics*, vol. 20, no. 12, p. 2050140, 2020.

[8] G. P. Warn and K. L. Ryan, "A review of seismic isolation for buildings: Historical development and research needs," *Buildings*, vol. 2, no. 3, pp. 300–325, 2012.

[9] S. Elias and V. Matsagar, "Research developments in vibration control of structures using passive tuned mass dampers," *Annual Reviews in Control*, vol. 44, pp. 129–156, 2017.

[10] S. Korkmaz, "A review of active structural control: Challenges for engineering informatics," *Computers and Structures*, vol. 89, no. 23–24, pp. 2113–2132, 2011.

[11] N. Fisco and H. Adeli, "Smart structures: Part I — Active and semi-active control," *Scientia Iranica*, vol. 18, no. 3A, pp. 275–284, 2011.

[12] M. D. Symans and M. C. Constantinou, "Semi-active control systems for seismic protection of structures: A state-of-the-art review," *Engineering Structures*, vol. 21, no. 6, pp. 469–487, 1999.

[13] J. N. Potter, S. A. Neild, and D. J. Wagg, "Generalisation and optimisation of semi-active, on-off switching controllers for single degree-of-freedom systems," *Journal of Sound and Vibration*, vol. 329, no. 13, pp. 2450–2462, 2010.

[14] M. Ostrowski, A. Jedlińska, B. Popławski, B. Blachowski, G. Mikułowski, D. Pisarski, and Ł. Jankowski, "Sliding mode control for semi-active damping of vibrations using on/off viscous structural nodes," *Buildings*, vol. 13, no. 2, 2023.

[15] J. Onoda and K. Minesugi, "Semiactive vibration suppression of truss structures by coulomb friction," *Journal of Spacecraft and Rockets*, vol. 31, no. 1, pp. 67–74, 1994.

[16] A. A. Ferri and B. S. Heck, "Analytical investigation of damping enhancement using active and passive structural joints," *Journal of Guidance, Control, and Dynamics*, vol. 15, no. 5, pp. 1258–1264, 1992.

[17] L. Gaul, J. Lenz, and D. Sachau, "Active damping of space structures by contact pressure control in joints," *Mechanics of Structures and Machines*, vol. 26, no. 1, pp. 81–100, 1998.

[18] L. Gaul and R. Nitsche, "The role of friction in mechanical joints," *Applied Mechanics Reviews*, vol. 54, no. 2, pp. 93–106, 2001.

[19] G. Mikułowski, B. Poplawski, and Ł. Jankowski, "Semi-active vibration control based on switchable transfer of bending moments: Study and experimental validation of control performance," *Smart Materials and Structures*, vol. 30, no. 4, p. 045005, 2021.

[20] B. Poplawski, G. Mikułowski, R. Wiszowaty, and Ł. Jankowski, "Mitigation of forced vibrations by semi-active control of local transfer of moments," *Mechanical Systems and Signal Processing*, vol. 157, 2021.

[21] M. Ostrowski, B. Blachowski, B. Poplawski, D. Pisarski, G. Mikulowski, and L. Jankowski, "Semi-active modal control of structures with lockable joints: general methodology and applications," *Structural Control and Health Monitoring*, vol. 28, no. 5, 2021.

[22] K. D. Young, V. I. Utkin, and Ü. Özgüner, "A control engineer's guide to sliding mode control," *IEEE Transactions on Control Systems Technology*, vol. 7, no. 3, pp. 328–342, 1999.

[23] M. Michajłow, Ł. Jankowski, T. Szolc, and R. Konowrocki, "Semi-active reduction of vibrations in the mechanical system driven by an electric motor," *Optimal Control Applications and Methods*, vol. 38, no. 6, pp. 922–933, 2017.

[24] B. Poplawski, G. Mikułowski, A. Mróz, and Ł. Jankowski, "Decentralized semi-active damping of free structural vibrations by means of structural nodes with an on/off ability to transmit moments," *Mechanical Systems and Signal Processing*, vol. 100, pp. 926–939, 2018.

[25] H. Lee and V. I. Utkin, "Chattering suppression methods in sliding mode control systems," *Annual Reviews in Control*, vol. 31, no. 2, pp. 179–188, 2007.

[26] G. Suwała and Ł. Jankowski, "A model-free method for identification of mass modifications," *Structural Control and Health Monitoring*, vol. 19, no. 2, pp. 216–230, 2012.

[27] M. Zawidzki and Ł. Jankowski, "Optimization of modular Truss-Z by minimum-mass design under equivalent stress constraint," *Smart Structures and Systems*, vol. 21, no. 6, pp. 715–725, 2018.

[28] A. Jedlińska, D. Pisarski, G. Mikułowski, B. Błachowski, and Ł. Jankowski, "Semi-active structural control using viscous dampers and reinforcement learning," in *10th ECCOMAS Thematic Conference on Smart Structures and Materials, SMART 2023*, 2023, pp. 1–8.